Journal of the Korean Electrochemical Society
Vol. 24, No. 1, 2021, 1-6
https://doi.org/10.5229/JKES.2021.24.1.1

Research Paper
pISSN 1229-1935
eISSN 2288-9000

New Design of $Li[Ni_{0.8}Co_{0.15}Al_{0.05}]O_2$ Nano-bush Structure as Cathode Material through Electrospinning

Yun-Chae Nam, Seon-Jin Lee, Hae-In Kim, and Jong-Tae Son*

Department of Nano-Polymer Science & Engineering Korea National University of Transportation, 50, Daehak-ro, Daesowon-myeon, Chungju-si, Chungcheongbuk-do, Republic of Korea

(Received September 1, 2020 : Revised February 3, 2021 : Accepted February 6, 2021)

Abstract : In this study, new morphology of NCA cathode material for lithium ion batteries was obtained through the electrospinning method. The prepared NCA nanofibers formed a nano-bush structure, and the primary particles were formed on the surface of the nanofibers. The embossing primary particles increased the surface area thus increasing the reactivity of lithium ions. The nano-bush structure could shorten the Li^+ diffusion path and improve the Li^+ diffusion coefficient. Scanning electron microscopy (SEM) revealed that the synthesized material consisted of nanofibers. The surface area of the nanofibers increased by primary particles was measured using atomic force microscopy (AFM). X-ray diffraction (XRD) analysis was carried out to determine the structure of the NCA nanofibers.

Keywords : Li-ion batteries, Cathode material, Electrospinning, $Li[Ni_{0.8}Co_{0.15}Al_{0.05}]O_2$

1. Introduction

Lithium-ion batteries (LIBs) are promising and widely used as electrochemical power sources for home appliances, electric vehicles (EVs), hybrid electric vehicles (HEVs), and energy storage devices.[1] Cathode materials significantly influence the electrochemical performance of LIBs, and a lot of effort has been in the development of high-performance cathode materials.[2,3] Nickel-rich layered metal oxides have attracted considerable attention owing to their ease of manufacture, low cost, non-toxicity, and high energy density.[4,5]

Among Ni-rich layered cathode materials, the $Li[Ni_{0.8}Co_{0.15}Al_{0.05}]O_2$ (NCA) is promising because of its superior structural stability and high capacity.[2-5] In particular, many synthetic methods, such as spray drying,[6] cation exchange,[7] spray pyrolysis,[8] sol-gel,[9] solution combustion,[10] and co-precipitation[11-13] have been used to prepare NCA. However, there are only a few reports on the synthesis of NCA nano fiber.[14]

*E-mail: jt1234@ut.ac.kr

We synthesized NCA nanofibers with novel nano-bush structures using the electrospinning method and simplified sintering process and analyzed the properties of the new nano-bush structure. The nano-bush structure, which is firmly connected to each other, is expected to improve the cycle life by preventing the fibers from cracking during cycle progress.

SEM confirmed that the nanofibers formed a nano-bush structure. In addition, the embossed primary particles were found to be the result of AFM and the surface area increased. The nano-bush structure improved the Li^+ diffusion coefficient by shortening the Li^+ diffusion path, while the embossed primary particles increased the surface area to increase the reactivity of lithium ions.

2. Experimental

2.1. Preparation of the electrospinning solution

The electrospinning solution was prepared using $LiNO_3$ (Aldrich), $Ni(NO_3)_2{\cdot}6H_2O$ (Aldrich, 98%), $Co(NO_3)_2{\cdot}6H_2O$ (Aldrich, 98%), $Al(NO_3)_3{\cdot}9H_2O$ (Aldrich, 99%), Polyvinylpyrrolidone (PVP)

(Aldrich), deionized water, CH_3OH (SK chemical, 99.99%), and HNO_3 (Aldrich, 99.999%). The mixed solution was stabilized for 24h before electrospinning.

2.2 Electrospinning

The prepared solution was placed in a plastic capillary. A stainless alloy was used as the collector. The distance between the capillary and the collector was set at 15 cm, and the applied voltage was 10-18 kV. The nanofibers were deposited on the collector, which was dried at 100°C for 24 h. The dried fibers were calcined at 750°C for 10 h in an O_2 atmosphere at a heating rate of 3°C/min.

2.3. Characterization

XRD of the cathodes were obtained using a Siemens D-5000 diffractometer in the 2θ range from 10° to 70° with Cu Kα radiation (λ = 1.54068 Å). The morphology of the obtained fibers was observed using SEM (JSM–7610F) and AFM (Bruker, multimode-n3-am).

For electrochemical testing, the cathode was fabricated by blending 80% active material, 10% super P carbon black, and 10% binder (10 wt% Polyvinylidenefluoride in 90 wt% *N*-methyl-2-pyrrolidone). The mixed slurry was cast uniformly on a thin Al foil and dried in vacuum for 12 h at 120°C. After drying, the film was pressed using a pressing machine at a pressure of 35 kgf/cm^2.

The electrochemical performance was measured using a CR2032 coin-type cell. A lithium-metal foil was used as the anode. The CR2032-type coin cells were assembled in a glove box, using the aforementioned anode film, lithium, a porous polypropylene film, and 1 M LiPF6 solution in a 3:7 volume ratio of ethylene carbonate (EC)/ diethyl carbonate (DEC). The lithium-metal foil was used as both the counter and reference electrodes. The cell was assembled in an argon-filled glove box. The initial charge-discharge and cycle capability were evaluated at a voltage that ranged from 3.0 to 4.3 V. The frequencies were changed from 0.001 Hz to 0.1 MHz, at an alternating-current signal amplitude of 10 mV. Nyquist plots (*Z' vs. –Z"*) were prepared and analyzed using Z-plot and Z-view packages.

3. Results and Discussion

The optical microscope image of the precursor of NCA (a) and the SEM image of the NCA cathode material (b) – (d) are shown in Fig. 1. The precursor had a smooth fiber shape, and after calcination, it contained nano-sized primary particles and retained its fiber shape. These primary particles were formed by the carbonization of PVP during the high-temperature heat-treatment process.[15)]

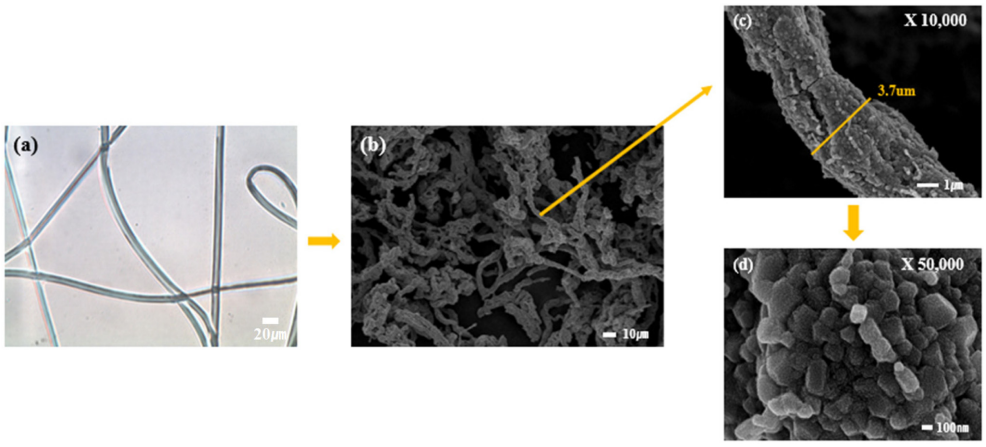

Fig. 1. (a) Optical microscope image of the precursor and (b)-(d) SEM images of the NCA nano-bush structure cathode materials.

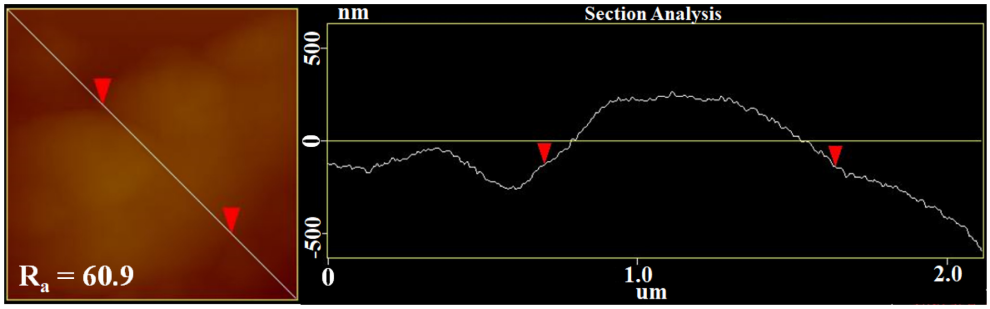

Fig. 2. AFM image of NCA nano-bush structure cathode materials.

The AFM data demonstrate the roughness of the nanofibers. Fig. 2 shows the atomic force microscopy (AFM) image of the $LiNi_{0.8}Co_{0.15}Al_{0.05}$ nanofiber after calcination at 750°C. Section Analysis was performed to confirm the fiber surface morphology and roughness. The roughness (R_a) value of the nanofiber was 60.9 nm. Primary particles were observed to be generated after calcination, and the surface area was found to increase.

Fig. 3 shows the XRD patterns of NCA after calcination at 750°C. All the major diffraction peaks were indexed as a layered oxide lattice based on a hexagonal α-$NaFeO_2$–type structure with the space group R-3m. The lattice parameters of the layered oxides were calculated to be a = 2.8654 Å and c = 14.1867 Å. The ratio I(003)/I(104) was calculated to be 1.23, indicating that the crystallinity was lower than that of conventional materials.[11-13)]

The electrochemical properties were analyzed using Fig. 4 (a, b) shows the initial charge-discharge curves and dQ/dV of NCA electrodes at a current density of 0.1 C, between 3.0 and 4.3 V. The initial discharge capacities of NCA

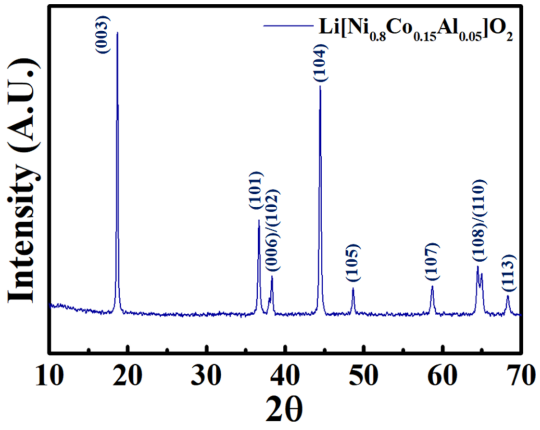

Fig. 3. XRD pattern of NCA nano-bush structure cathode materials.

were 168.7 $mAhg^{-1}$. In the case of conventional NCA, the discharge capacity is approximately 190 mAh/g at 0.1C,[11-13)] indicating that the capacity is higher than in this study. Fig. 4 (c) shows the initial discharge capacity of the NCA electrode. By the 100th cycle, NCA had decreased from 145.2 to 113.2 $mAhg^{-1}$. (Capacity retention = 78.0%). Compared to conventional NCA,[11-13)] the

Table 1. Lattice parameters of the NCA nano-bush structure cathode materials

Sample	a (Å)	c (Å)	V ($Å^3$)	$I_{(003)}/I_{(104)}$	R-factor
$Li[Ni_{0.8}Co_{0.15}Al_{0.05}]O_2$	2.865 (±0.002)	14.187 (±0.009)	100.87 (±0.016)	1.23	1.02

Table 2. Resistance of the electrolyte solution (R_s), surface film (R_{SEI}) and charge-transfer resistance (R_{ct}) of NCA nano-bush structure cathode material by Nyquist circles

Sample	R_s (Ω)	R_f (Ω)	R_{ct} (Ω)	Li diffusion coefficients (D_{Li})
Before cycle	2.2	229.2 (±0.4)	2,326.7 (±9.1)	1.3×10^{-15} cm^2/s
After 1 cycle	3.1	73.0 (±0.1)	639.6 (±0.9)	6.4×10^{-14} cm^2/s

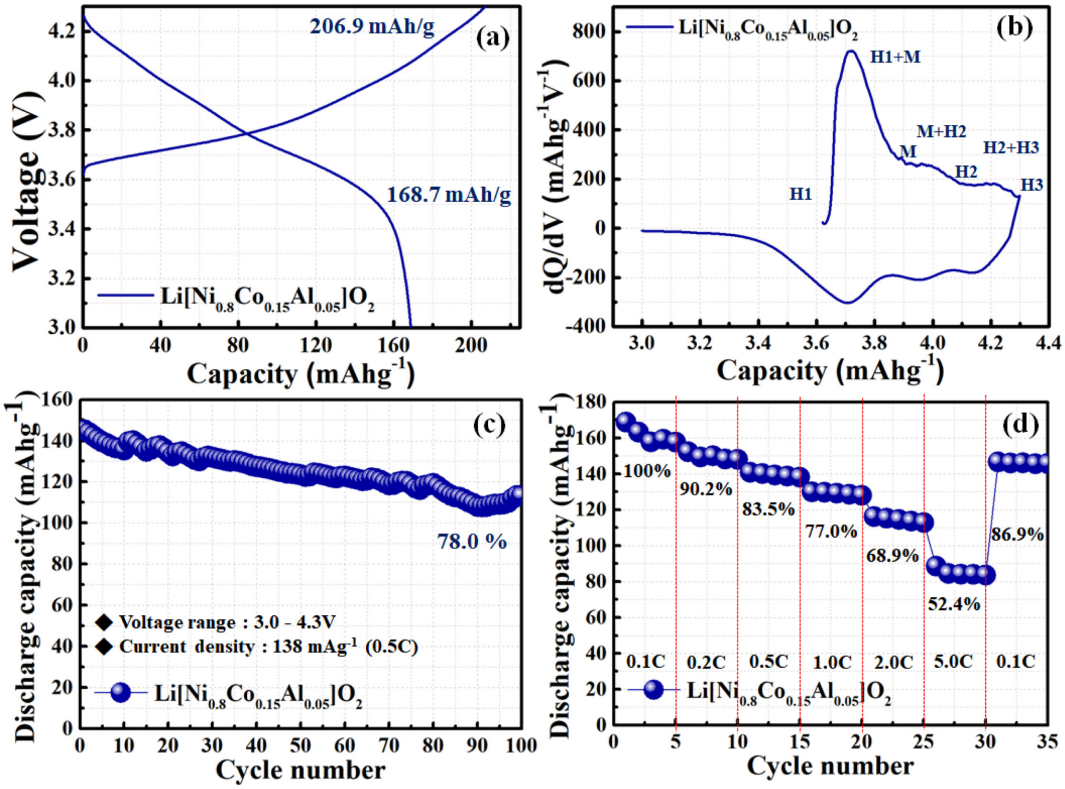

Fig. 4. (a) Initial charge-discharge curves and (b) differential capacity plots versus voltage of NCA nano-bush structure cathode materials in the voltage range of 3.0–4.3 V at 0.1 C. (c) Discharge capacities versus cycle number of NCA nano-bush structure cathode materials cycled in the voltage range of 3.0–4.6 V at 1 C. (d) Rate performance of NCA nano-bush structure cathode materials.

reduced capacity retention at 0.1C is presumed to be an increase in cation mixing. Fig. 4 (d) shows rate performance of NCA nano-bush structure cathode materials. The result can be found that the discharge specific capacity of NCA nano-bush structure can still remain ~112.8 mAh g^{-1} at 5 C.

Fig. 5 shows the AC impedance spectra of the NCA. The electrode data show the electrolyte solution resistance (R_s), solid electrolyte interphase (SEI) resistance (R_{SEI}), and charge transfer resistance (R_{ct}). Table 2 shows that The R_s, R_{SEI}, and R_{ct} of the NCA electrode were measured to be 2.2, 229.2, and 2326.7 Ω, respectively. After the cycle, the R_s, R_{SEI} and R_{ct} of the NCA electrode were measured to be 3.1, 73.0 and 639.6 Ω, respectively as shown Table 2. The nano-bush NCA showed significantly reduced impedance after cycle. This phenomenon shows a large resistance due to the stress of the cathode electrode due to high pressure roll pressing, and then stabilizes after one cycle and the resistance decreases.

EIS can be used to calculate the lithium diffusion coefficient (D_{Li}) using the following equations.

$$Z_{re} = R_{ct} + R_s + \sigma\omega^{-0.5} \quad (1)$$

$$D_{Li} = 0.5\left(\frac{RT}{AF^2\sigma_W C}\right)^2 \quad (2)$$

where R_{ct} is the charge-transfer resistance, ω the angular frequency in the low-frequency region, D the diffusion coefficient, R the gas constant, T the absolute temperature, F the Faraday's constant, A the area of the electrode surface, and C the

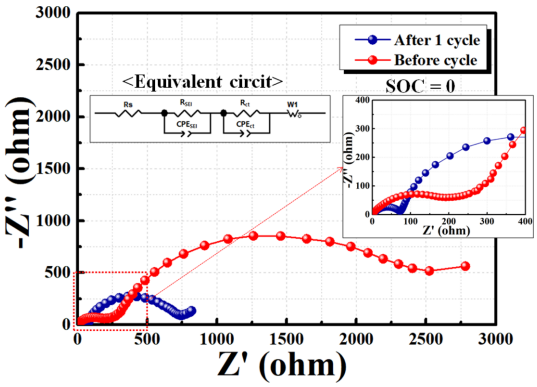

Fig. 5. Impedance plot of NCA nano-bush structure positive electrode before cell test and after 1 cycles at state of charge = 0.

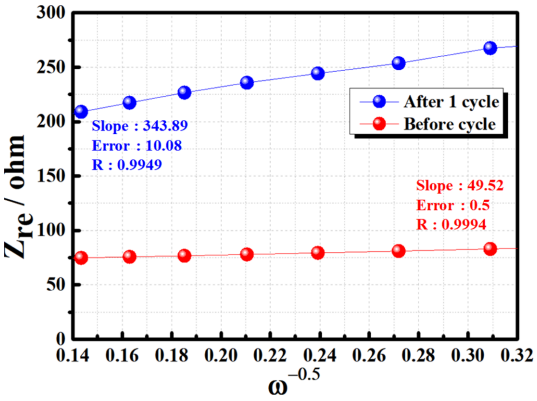

Fig. 6. Lithium diffusion coefficients of NCA nano-bush structure positive electrode before cell test and after 1 cycles at state of charge = 0.

molar concentration of lithium ions (moles/cm^{-3}).[16,17] The plot of Z_{re} versus the reciprocal square root of the lower angular frequencies is illustrated in Fig. 6. D_{Li} of the NCA nano-bush was 6.4×10^{-14} cm^2/s and higher than that of traditional NCA particles.[18] However, further studies are needed on the improved discharge capacity and cycle stability of nano-bush NCA.

4. Conclusions

Novel $Li[Ni_{0.8}Co_{0.15}Al_{0.05}]O_2$ nano-bush cathode materials were successfully synthesized through an electrospinning method. SEM confirmed that the nanofiber cathode material was composed of a nano-bush structure. After calcination at 750°C, the embossed primary particles were formed on the surface of the nanofiber. The surface area was increased by the primary particles by AFM, and the surface roughness was measured to be 60.86 nm. The cation mixing is lower than that of conventional materials because it is synthesized at low temperatures. The initial charge and discharge capacities were 138.13 mAh/g, and the discharge capacity of the NCA electrode was reduced from 145.2 mAh/g to 113.2 mAh/g by the 100^{th} cycle at 0.5 C. The nano-bush structure shortens the Li^+ diffusion path and improves the Li^+ diffusion coefficient. In addition, the formation of primary particles increased the surface area of the nanofibers to increase the reactivity of lithium ions. However, further studies are needed on the improved discharge capacity and cycle stability of nano-bush NCA.

Acknowledgments

This study was supported by financial resources granted by the Ministry of SMEs and Startups, Republic of Korea(S2928638) and the National Research Foundation of Korea (NRF) funded by the Korea government (MSIT, No. 2019R1F1A1057220) and by the Technology Innovation Program (or Industrial Strategic Technology Development Program-Material Parts Technology Development Project) (20003747, Development of high-performance cathode material manufacturing technology through valuable metal upcycling from waste battery and waste cathode material) funded by the Ministry of Trade, Industry & Energy (MOTIE, Korea) and the Korea Agency for Infrastructure Technology.

References

1. Y. Tang, Y. Zhang, W. Li, B. Ma, and X. Chen, *Chem. Soc. Rev.* **44**, 5926 (2015).
2. S. Xia, J.-J. Liu,., F. Li, F. Cheng, X. Li, C. Sun, and H. Guo, *Ceram Int* **44(8)**, 9294 (2018).
3. L. Qiu, W. Xiang, W. Tian, C-L. Xu, Y-C., Li, Z. G. Wu, and X. D. Guo, *Nano Energy,* **63**, 103818 (2019).
4. W. Liu, P. Oh, X. Liu, M. Lee, W. Cho, S. Chae, Y. Kim, and J. Cho, *Chem. Int. Ed.* **54**, 4440 (2015).
5. P. He, H. Yu, D. Lia, and H. Zhou, *J. Mater. Chem.* **22,**

3680 (2012).
6. Y. Chen, P. Li, S. Zhao, Y. Zhuang, S. Zhao, and Q. Zhou, *RSC Adv.* **7,** 29233 (2017).
7. W. Chen, Y. Li, D. Yang, X. Feng, X. Guan, and L. Mi, *Electrochim. Acta* **190,** 932 (2016).
8. S.H. Ju, H.C. Jang, and Y.C. Kang, *Electrochim. Acta* **52,** 7286 (2007).
9. C.J. Han, J.H. Yoon, W.I. Cho and H. Jang, *J. Power Sources*. **136,** 132-138. (2004).
10. S.B. Majumder, S. Nieto and R.S. Katiyar, *J. Power Sources.* **154**, 262-267 (2006).
11. H. Ouyang, X. Li, Z. Wang, H. Guo, W. Peng and Z. He, *Funct. Mater. Lett.,* **11** 1850083 (2018).
12. M. Liang, D. Song, H. Zhang, X. Shi, Q. Wang, and L. Zhang, *ACS Appl. Mater. Interface,* **9** 38567-38574 (2017).
13. H. Xie, K. Du, G. Hu, J. Duan, Z. Peng, and Z. Zhang, *J. Mater. Chem. A,* **3** 20236 (2015).
14. L. Zhang, Z. Zhao, X. Li, H. Fang, L. Wang, Y. Song, and X. Jia, *Mater. Res. Express*, 7, 015526 (2020).
15. J. J. Bae, J. W. Shin, S. J. Lee, S. J. Kim, T. W. Hong, and J. T. Son, *J. Nanosci. Nanotechnol*. **20(1)**, 338 (2020).
16. Cai, L., Liu, Z., An, K. and Liang, C., *Journal of The Electrochemical Society*, **159(7)**, 924-928. (2012).
17. Stoyanova, R., *Solid State Ionics*, **128(1-4)**, 1-10. (2000).
18. R. Chen, H. Zhang, J. Xie, Y. Lin, J. Yu, and. L. Chen, *Chem. Electro. Chem*, **5(21)**, 3176-3182, (2018).